An Efficient SEPIC-Zeta Converter with Adaptive Pi Controller for Grid Tied Applications

[1]A.R. GAYATHRI, [2]A.ANNIE STEFFY BEULA, [3]A. DARWIN JOSE RAJU,

[4]M. MARY SYNTHIA REGIS PRABHA D. M

[1]*Department of Electrical and Electronics Engineering, Stella Mary's College of Engineering, Tamilnadu, India, 629202*

[2] *Assistant Professor, Department of Electrical and Electronics Engineering, Stella Mary's College of Engineering, Tamilnadu, India, 629202*

[3] *Associate Professor, Department of Electrical and Electronics Engineering, St.Xavier's Catholic College of Engineering, Tamilnadu, India, 629003*

[4] *Associate Professor, Department of Electrical and Electronics Engineering, Noorul Islam Centre for Higher Education, Tamilnadu, India, 629180*

Abstract: *Using a dc-dc converter and a bidirectional ac-dc converter, the suggested system is capable of continually charging the EV battery regardless of solar irradiation. With the suggested bidirectional configuration in the charging system, SEPIC-Zeta converters are used for dc-dc converters, and Line commutated converters are employed as bidirectional ac-dc converters. During peak sunshine hours, extra PV array power is delivered to the single-phase utility grid in addition to charging the EV battery. During cloudy hours, the PV array electricity generated is solely used to charge the EV battery. During off-peak and overcast hours, the power grid supplied EV battery charging via a bidirectional ac-dc converter. For MPPT operation, a Remora Optimization and Fuzzy Logic Controller Algorithm based Adaptive PI Controller is implemented, which was designed in hardware with a DSPIC30F4011 controller. The system's dynamic characteristics are analyzed, and the corresponding results are also presented in this paper.*

Keywords: *Solar PV array, Electric vehicle, SEPIC–ZETA converter, Remora Optimization, Fuzzy Logic Controller and Adaptive PI Controller.*

Introduction

The entire region is advancing toward a source of energy that will never run out and will not hurt the environment [1, 2]. Conventional automobiles destroy the environment, and as a result, fossil fuels are depleted day by day. As a result, a solution to this problem is required, and Electric Vehicles (EV) is the best option [3, 4]. Solar energy is a clean source of energy that is available all year and may be utilized to power electric vehicles. Another issue is that solar energy alone is insufficient to operate the vehicle [5-7].

Various DC–DC bidirectional converters are utilised in practical situations to assist both the charging and draining of batteries. Buck-boost topology and Cuk converter are the primitive converters employed in this case [8-10]. SEPIC and Zeta converter in the Battery Energy Storage System is anticipated to properly perform its dynamic regulating action so that charging and discharging currents promptly settle to the matching optimal values even with fewer transient peaks.For the aforementioned converter, an adaptive fuzzy based proportional-integral (PI) based control loop is first established, and evaluation converters are being developed in the future for their benefits, as stated in the paper. Because it can operate within a wider range of BESS operation, the united SEPIC-Zeta bipolar DC-DC converter is used in this study. The bidirectional SEPIC-Zeta converter also has smaller current and voltage ripples compared to previous bidirectional converters [11–14]. The DC-DC bidirectional of the different dynamic responses during charging and discharging operations [15-17]. The use of the described Remora optimization approach considerably improved these responses. As a result of the smooth charging and discharging profile established, the battery's life span can be extended. Furthermore, the recommended technique is adaptable to changing operational conditions throughout charging and discharging cycles [18-19]. Alternatively, retuning of PI controller gains is required under changed operating conditions, however it is extremely difficult to achieve under unpredictable changeable situations.As far as the investigator is conscious, there hasn't been any published research on the dynamic performance of SEPIC-Zeta converter-based Battery Energy Storage System during charging and discharging cycles [20]. Further from that, this study's new contribution is the use of remora optimization with fuzzy based adaptive PI controller to improve the dynamic behaviour of the system in question. This project focuses on using solar energy to generate electricity. Solar energy can be used in a variety of ways. This project will provide an overview of the solar photovoltaic principle, the components and workings of a solar photovoltaic system, how to maintain a solar photovoltaic system, and the history of solar energy use worldwide. The following is the overview of the paper: The description of theRecentResearch Work is presented in segment 2. Segment 3 describes the suggested proposed system model. The control system design is presented in Section 4. In segment 5, the tentative results were discussed. The conclusion is obtainable in Section 6.

A Review of Recent Research Work

The literature has already published a variety of research efforts on charging electric vehicles using a PV integrated grid with diverse approaches and aspects. Here, a few of them are discussed.

The ideal adaptation law for any type of flexible energy conservation plan (ECMS) for plug-in HEVs operating in charge-reduction form have been provided by Rezaei et al. [21]. A specific adaptive ECMS, called as catch energy saving opportunity, is chosen to present the ideal legislation (CESO). CESO was originally introduced in charge-sustaining mode for series and parallel HEVs.Here, the best adaption law is proposed, expanding CESO approach to plug-in HEVs in charge-exhaustion form.

A vigorous pole assignment yaw regulator with parametric uncertainty was used by Ni et al. [22]. A full XBW electric car testing is used as an illustration to show how the CCV improves hardware configuration flexibility. At facilitate assembling, save space, and enhance the arrangement of the electric wires, all XBW apparatus can be generously located to any position under the CCV. The CCV illustrates the interaction and mutual benefit of mechanical parts and electric control systems through the analysis of yaw moment requirement in various scenarios. Based on the findings, experiments show that the proposed yaw controller has a suitable efficiency. The UGV's C.G position has much more variety now, which enhances the vehicle's capacity for closed-loop driving. The aircraft's general structure is influenced by the electric control system.

To solve the multimode integration function with actuator faults in a 4WID system, Zhang et al. [23] developed adaptive sliding mode (ASM) control and fault-tolerant (FT) control allocation. Earliest, a new vehicle dynamics model with a deformable driver motor is developed. An adaptive variable exponential reaching law is used in the ASM control layer to reduce crosstalk and get better reaching speed, accuracy, and robustness. The four in-wheel motors are then appropriately coordinated using the FTC allocation, which is built via quadratic programming, when the motor fault occurs. If the actuator malfunctions when the vehicle is moving at a high speediness on a low friction road, a major traffic collision could happen.

Regarding the operational safety of EVCS, Wang *et al* [24] concentrated on three key areas: (1) facility degradation, which may affect EVSE reliability concert and EVCS safeguardmalfunction; (2) When smart charging and communication between EVCSs and electric utilities are enabled, cyber-attack issues arise; and (3) there is a possible discrepancy between renewable output and EVCS demand. This might generate system steadiness. The suggested approach will give EVCS operators helpful guidelines for continued oversight management for usual EVCS operations.

Description of System with Proposed Converter

The structure of the proposed method is represented in Figure 1. The EV charging station system is a self-contained charging station powered by a solar panel. The PV panel, on the other hand, turns the solar energy absorbed by the insulation into electrical energy, which is then fed to the EV charging station. The PV output is connected to a boost regulator. The DC link voltage is matched to the PV output voltage by this device. It is also utilised to ensure that the PV array's maximum power point tracking (MPPT) status is maintained. Two DC/DC converters are connected to the DC bus. SEPIC-Zeta converters and Line commutated converters are the names of the converters. The general explanation of BESS is examined in this suggested system, which permits both battery charging and discharging via the DC bus. Battery energy storage system is made up of a rechargeable battery and a SEPIC-Zeta bipolar DC–DC converter. In this method, the SEPIC configuration is active when the battery is being discharged, and the Zeta configuration is activated when the battery is being charged. Following that, the battery and operational modes of proposed system are explored:

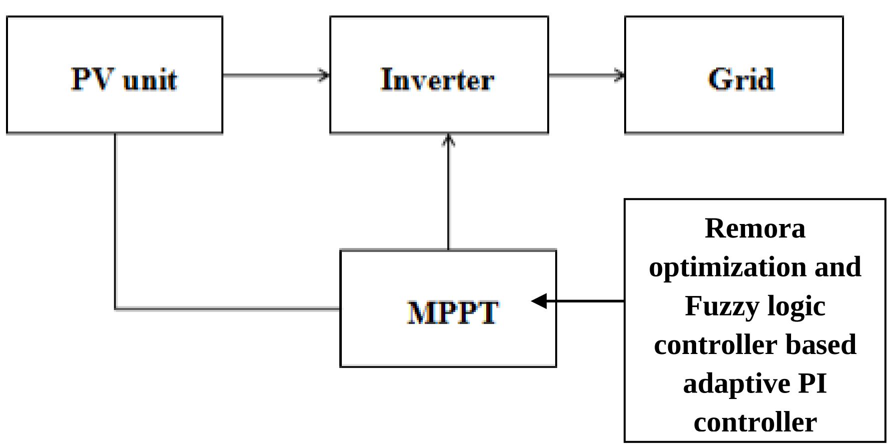

Figure 1:Block diagram of a grid load -connected PV system

 https://doi.org/10.37896/pd91.4/91489

ISSN: 0369-8963

Battery charger

The state of charge (SOC) of a battery is an essential parameter to monitor before deciding when and how to start charging and discharging it. The SOC number of zero percent indicates that the battery is completely depleted and needs to be charged right away. On the other hand, a SOC rating of 100 percent indicates that the battery is completely charged and ready to discharge at maximum capacity.

Methods of operations

Charging and discharging are the two modes of operation for the proposed system converter. The following is a basic overview of the charging process:

Mode1:

This section discusses the practical circuit diagram of the charging mode, which is implemented by turning on the switch "Sa" and the anti-parallel diode "Dz". During charging, the circuit arrangement acts as a zeta converter. This circuit design works like a buck converter as it uses a conventional DC bus voltage higher than the battery voltage as the input voltage throughout the charging process. During this case, the duty ratio (D_{R1}) of the Pulse Width Modulation signal is changed for the switch "Sa" to sustain the required voltage at the battery terminal and supply the appropriate charging current to the battery. The voltage relationships between the input and output of a zeta converter are as follows:

$$B_{vol} = \frac{D_{R1}}{1-D_{R1}} V_{in\_out} \tag{1}$$

For the zeta converter to perform buck operation in charging mode, the regulated value must be less than 0.5. The battery discharge process is explained in detail as follows:

Mode 2:

The switch "Sb" and the anti-parallel diode "Ds" must be activated in order for the circuit diagram to function effectively in this mode of operation. The circuit arrangement resembles a SEPIC converter as a result.The converter operates as a boost converter by stepping up the battery voltage (which is the SEPIC converter's input voltage) to the controlled output voltage after the discharged current has been transmitted to the DC bus through SEPIC design. The duty ratio (D_{R2}) of the Pulse Width Modulation signal from switch "Sb" is adjusted to change the converter's output voltage, which in turn affects how much current is discharged. The input-output correlation of the SEPIC converter is as follows when it is operating in the discharging mode:

$$V_{in\_out} = \frac{D_{R2}}{1-D_{R2}} V_{pv} \tag{2}$$

https://doi.org/10.37896/pd91.4/91489

The inhibited value of D_{R2} is standard to be more than 0.5 in this case to retain the SEPIC configuration's boost operation.

Control Methodology using various optimizations

The remora optimization based fuzzy with adaptive PI controller is utilized in this proposed approach to track the maximum power from solar panel and to switch the sepic-zeta bidirectional converter. Following is a discussion of a full description of control methods:

Overview of ROA

Remora can save energy by swimming on whales, which also keeps her safe from opponent attacks. When the ocean is stuffed with food, the remora detaches from the host (the whale) and after ingestion and digestion of food, moves it to a higher position and moves to a differentoceanic component. The parts that follow discuss free travel modelling and intelligent remora feeding in various remora circumstances.

Initialization

The position of the candidate's response in the explore space is chosen as a difficulty variable, and the candidate's reaction is treated as a remora in the ROA. The remora moves around in one-dimensional space as it ascends to the top. The remora is actually stationed as follows:

$$re_i^{t+1} = re_b^{\ t} - \left(rand(0,1) * \left(\frac{re_b^{\ t} + re_{rand}^{\ t}}{2} \right) - re^t{}_{rand} \right) (3)$$

$$re_i = (re_{i1}, re_{i2}, re_{i3}, ...re_{id}),$$

Where, the remora number is i, and the dimension is d, correspondingly.

In other words, in the biological behavior of the remora, $re_b = (r_1, r_2, ...r_d)$ denotes the food (target), signifying the best remedy for the ROA. Every answer in the ROA possesses competency fitness.

Exploration

• Swordfish optimization approach

The remora's location is updated if it maintains engaged to the swordfish. Its model for updating its location is described as follows, where t is the present iteration, T denotes the highest number of iterations, and r_p denotes a position that was randomly selected. The exploration of the search space is also required for the random selection of remora. The remora's choice of host is determined by whether or not the host has eaten the prey. To put it another way, the present qualifying rate is higher than the preceding generations.As a result, the history of the attack is used to determine the competency's present value. The remora ding to the must continuously makes minor movements in the vicinity of the host, deciding whether to change the host or not depending on their level of fitness. A good example of this behavior is as follows:

$$r_a = r_{ti} + (r_{ti} - r_p) \times rand_n \quad (4)$$

r_{ti} and r_a denote the previous generation's position and the test step, respectively. Similarly, rand n indicates the remora's modest global step taken at random.The host will then either change at random or not, as determined by the remora. Alternatively said, the fitness values of the tested response and the current reaction are contrasted. The remora selects one of several eating techniques for narrow optimization in this circumstance.

$$f(r_{ti}) \rangle f(r_a) \quad (5)$$

$$f(r_{ti}) \langle f(r_a) \quad (6)$$

One Whale Optimization Algorithm (WOA) Strategy for Thoughtful Nutrition (Exploitation)

The location of the whale's linked remora is being updated, according to the WOA.

$$r_{i+1} = D_1 \times \exp a \times \cos(2\pi\beta) + r_i \quad (7)$$

$$\beta = rand(0,1) * (a-1) + 1 \quad (8)$$

The distance among the hunter and the victim is denoted by D. α = ranis a digit chosen at random between 1 and 1. Is a number that ranges between 1 and 2, and the number of iterations that can be used as follows,

$$a = -\left(1 + \frac{t}{t_{\max}}\right) \quad (9)$$

$$D_1 = |r_b - r_i| \quad (10)$$

The host's position space can be used to confine the response space. Short-step movement in the host space is described as follows:

$$r_i^t = r_i^t + P \quad (11)$$

$$P = Q \times r_i^t - R \times r_b \quad (12)$$

$$Q = 2 \times v \times rand(0,1) - v \quad (13)$$

https://doi.org/10.37896/pd91.4/91489

ISSN: 0369-8963

$$v = 2 \times \left(1 - \frac{t}{t_{\max}}\right) \quad (14)$$

where P denotes the narrow distance between the fish adhesive and the host. To denote its position, R stands for the coefficient of stickiness, which is in the range of [0, 0.3].

In MPPT solving via the ROA, power of the PV system is formulated as follows:

$$ROA = P_{pv\_\max}(d) \quad (15)$$

The optimization variable (d) is constrained by:

$$d_{\min} \langle d \langle d_{\max} \quad (16)$$

In this work, the d of the converter of the PV system was ideally adjusted using the ROA as a direct control method to lessen oscillations in the system steady state. The following are the steps to apply the ROA in order to solve the MPPT problem:

Step (1) Information about ROA is entered in this stage. The duty cycle's smallest and highest intervals are also utilized.

Step 2: For each population, a random duty cycle is generated using the ROA, voltage, and ensuing current. This random duty cycle is then utilised to determine the PV power for that population. Step 3: The best agent for the algorithm is chosen, and this is the agent with the maximum PV power in step 2.

The following equations are used to update the ROA population set (d) in accordance with the ROA's exploration and exploitation phases:

$$d_i^{t+1} + L_i = d_i^t + \left(2 \times \left(1 - \frac{t}{t_{ma}}\right) \times \left(2 \times rand(0,1) - 1\right) \times \left(d_i^t \times (1 - R)\right)\right) \quad (17)$$

where d_i^{t+1}I refer to the duty cycle in $t+1$iteration related to i^{th} remora and t is the ROA iteration number.

Furthermore, using the ROA-based MPPT issue, the PV system power is described as follows:

$$P_{pv}(d(t+1)j,k) \rangle P_{pv}(d(t)j,k) \quad (18)$$

Step (5) calculates the PV power for the revised population using the goal function (selection of new duty cycles).

ISSN: 0369-8963

Step (6) The best agent with the highest influence from step 5 is selected as the population representative. Step 3 should not be used if the alternative solution is better.

Step (7) Proceed to step 8 if the convergence conditions—to get maximum power and perform the maximum number of ROA repetitions—are satisfied; if not, proceed to step 4.

Additionally, at this point, changes in the climate have an impact on the PV system's output power. To get to the GMPP, the ROA population needs to be re-quantified as follows:

$$A(R\_t+1)P_{pv} - A(R\_t)P_{pv} \times A(R\_t)P_{pv} \geq \Delta A \quad (19)$$

Step (8) the conclusion (achieving maximum power and determining the optimal duty cycle).

PI algorithm with fuzzy parameters

Fuzzy control, which is related on language rules and fuzzy inference, is an important subfield of intelligent control in current control theory. The adaptability of fuzzy control is advantageous. The benefit of fuzzy control is that it does not necessitate learning a perfect mathematical model of the controlled item; instead, it relies on the knowledge of the workers or experts to set up the control judgment table, construct the control rules, and then pick the size of the control quantity. The fuzzy controller in this study consists of two-dimensional system, deviation E, and deviation change rate ec and PI parameter correction values K_p and K_i as input variables and modified as output variables using fuzzy control rule.The set of fuzzy conditional statements that make up the fuzzy control rule are the result of the expertise and skills of experts and operators. The key to a successful fuzzy controller is formative the appropriate fuzzy control rules that will allow the system to attain the required active and inactive characteristics. The following are the self-tuning regulations for fuzzy PI parameters K_p and K_i in general:

i) When the framework deviation e is considerable, the greater K_p and K_i should be used to fulfill the goal of reducing the system deviation e as quickly as feasible, regardless of the deviation change rate ec symbol deviation.

ii) If the deviation e is moderate, a lower K_p should be used, and K_i should be set to a medium value to avoid the system from overshooting.

iii) When the framework deviation e is modest or zero, a moderate K_p and a small K_i may the fuzzy rules of K_p and K_i are established related to the fuzzy PI parameter fine-tuning principle.

To acquire the output surface of K_p and K_i, the suitable membership function and method can be determined based on the fuzzy rule, fuzzy variable, and fuzzy domain be used to reduce the system's adjustment time.

Result and Discussion

The experimental setup is specifically intended to be controlled by the dsPIC30F motor control family. Compared to standard PIcontrollers, dsPICs process data at a substantially faster rate. It has high speed analogue to digital converters and a motor control pulse width modulation (MCPWM) module. Eight output pins and six PWM generators make up the MCPWM modulator. The required mathematical operations are supported by the DSP engine of the dsPIC30F4011. It has an analogue to digital converter with 10 bits and 1 MSPS. The schematic diagram of the dsPIC30F4011 controller is shown in Figure.2.

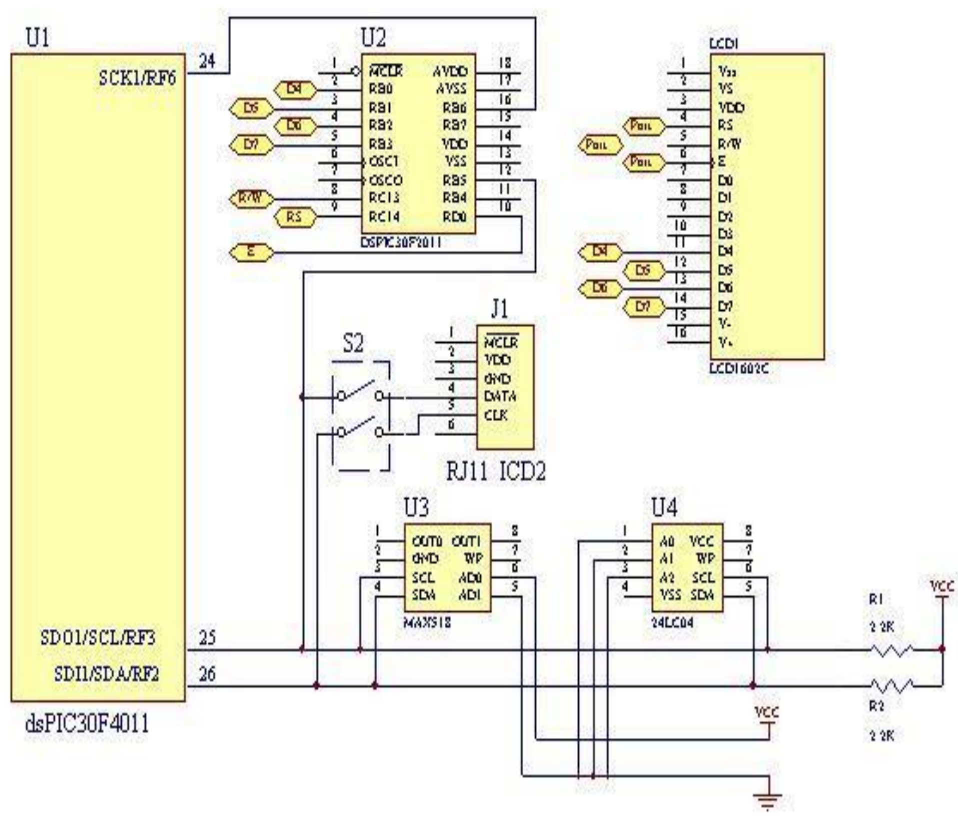

Figure 2:Schematic of DSPIC 30F4011 controllers

The controller has an integrated DSP mechanism with double data fetch and accumulation engrave-back for DSP functions.

• Bit-Reversed Addressing and modulo modes.

• Two accumulators, each 40 bits wide, with configurable saturation logic.

• Each and every DSP instruction is one cycle.

• Hardware fractional/integer multiplier with a single cycle of 17 bits. The motor control PWM module of the controller has particular functionality.

 https://doi.org/10.37896/pd91.4/91489

• 6 channels for PWM output. Output modes that are complementary or independent aligned-edge and -centre modes.

• 3 generators with a duty cycle.

• Output polarity can be programmed.

• Complementary mode Dead-time control.

• Control of manual output.

• A/D conversions trigger.

Experimental Analysis

The SEPIC-ZETA converter and fuzzy adaptive PI controller with remora optimization are utilised in the proposed system to get the most power out from the PV system. Additionally, it is used to supply the Grid with the DC output voltage of the converter converted to AC power using a single phase voltage source inverter. Additionally, the proposed system is implemented using hardware, and the following experimental findings and discussions are provided.

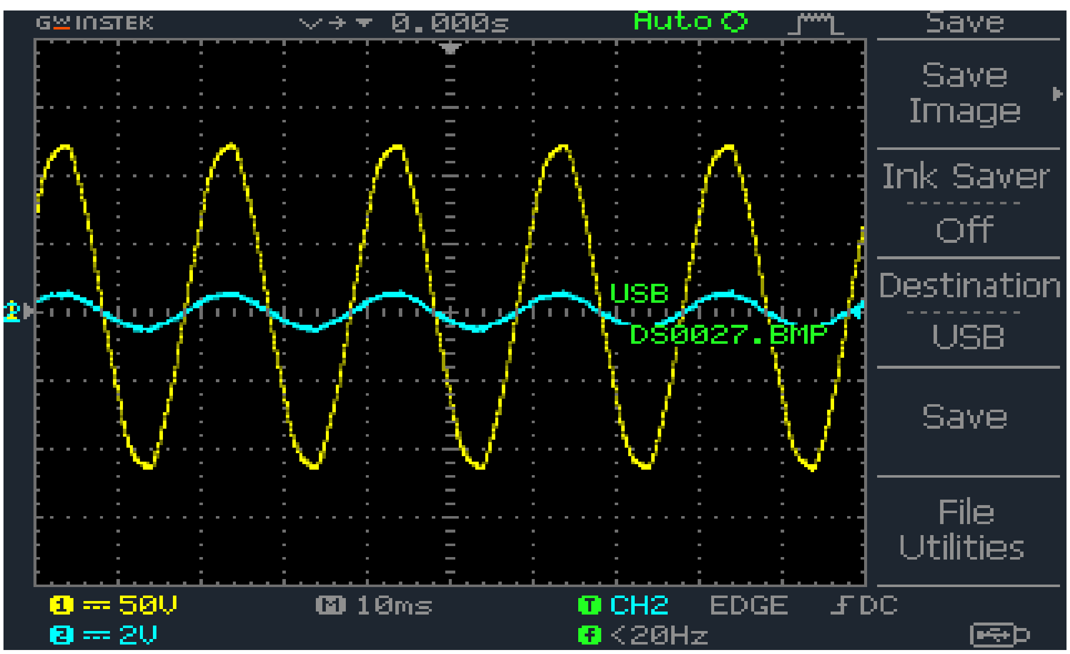

Figure 3: Input supply AC Waveform

https://doi.org/10.37896/pd91.4/91489

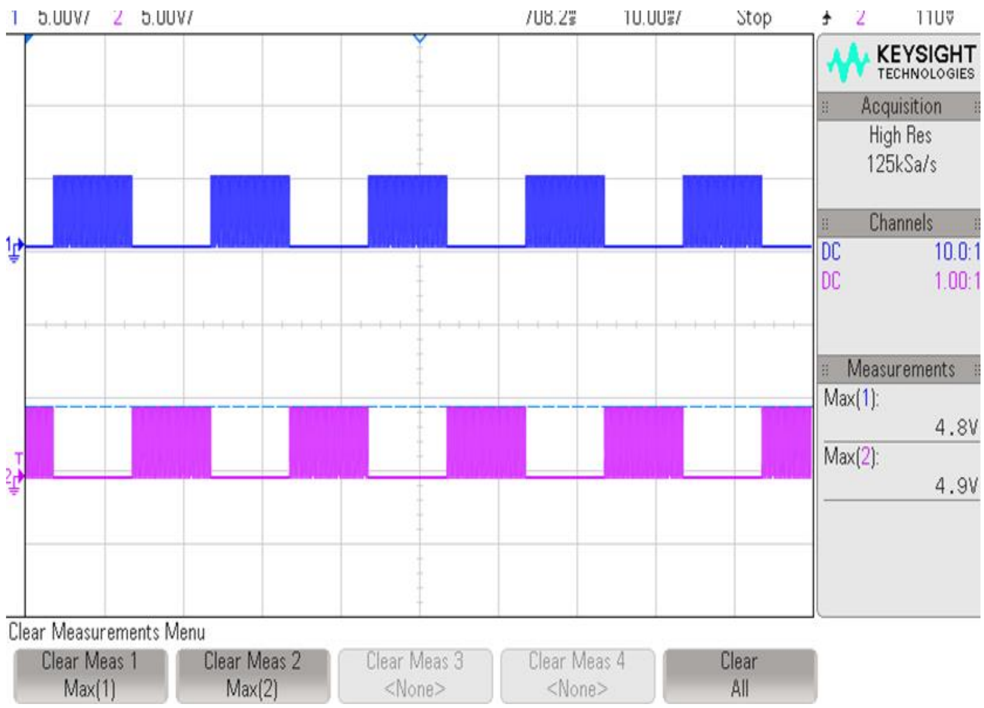

Figure 4:PWM Pulses to the Converter

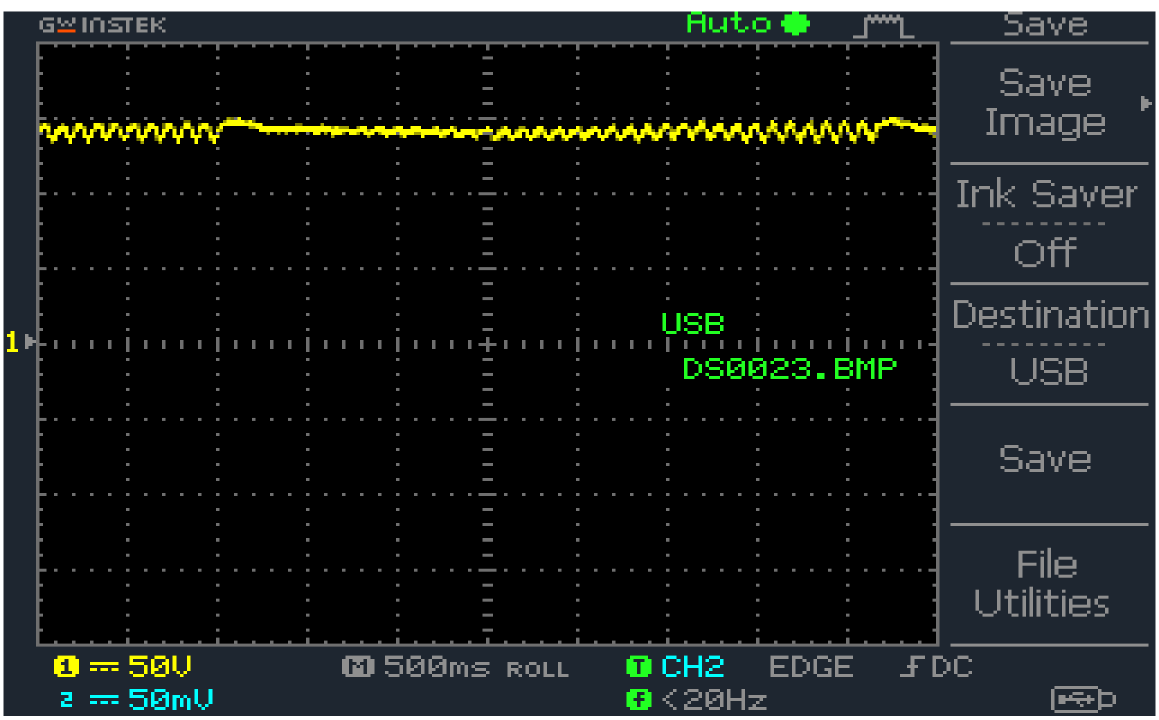

Figure 5:DC voltage waveform generated by converter

 https://doi.org/10.37896/pd91.4/91489

ISSN: 0369-8963

The aforementioned schematic displays the experimental outcomes of the suggested system, with fig. 3 implying the bidirectional converter's alternating current input supply and fig. 4 illustrating the pulse input of the SEPIC-ZETA converter. Finally, the converter's output is displayed. This is a dc waveform that has been converted to an ac wave and will be fed into the grid. Track the maximum power coming from the photovoltaic system, which is then converted to an AC waveform using one of the given control methodologies. Next, the suggested converter produces a DC waveform as an output, which is then supplied to the grid system or load.

Conclusion

This method deals with the integration of SEPIC-ZETA converters and a 1 bidirectional inverter for EV charging applications. The output voltage of a DC-DC converter might be less than, equal to, or greater than the input voltage. A one-volt bidirectional inverter is used to convert DC voltage to AC voltage. Bidirectional inverters use PWM signals to convert DC to AC voltages when operating in grid-connected mode. DC loads typically operate more efficiently than Alternating Current loads because the coordination of AC loads necessitates synchronizing the recurrence of AC-AC converters with grid synchronization, power factor, and grid stability difficulties.

REFERENCES

1. Alanazi, A., Alanazi, M., Arabi, S. and Sarker, S., 2022, ‘A New Maximum Power Point Tracking Framework for Photovoltaic Energy Systems Based on Remora Optimization Algorithm in Partial Shading Conditions’, Applied Sciences, vol.12, no.8, p.3828.
2. Cheikh-Mohamad, S., Sechilariu, M. and Locment, F., 2022, ‘Real-Time Power Management Including an Optimization Problem for PV-Powered Electric Vehicle Charging Stations’, Applied Sciences, vol.12, no.9, p.4323.
3. Das, B., Panigrahi, P.K., Das, S.R., Mishra, D.P. and Salkuti, S.R., 2022, ‘Power quality improvement in a photovoltaic based microgrid integrated network using multilevel inverter’, International Journal of Emerging Electric Power Systems, vol.23, no.2, pp.197-209.
4. He, L., Li, F., Guo, C., Gao, B., Lu, J. and Shi, Q., 2022, ‘An Adaptive PI Controller by Particle Swarm Optimization for Angle Tracking of Steer-by-Wire’, IEEE/ASME Transactions on Mechatronics.
5. ISAH, H., Yunusa, A. and Hajara, M.A., 2022, ‘An Extended Sepic DC-DC Converter for Micro-Grid Based Photovoltaic (Pv) Applications’.
6. Jia, H., Peng, X. and Lang, C., 2021, ‘Remora optimization algorithm’, Expert Systems with Applications, 185, p.115665.
7. Kumar, M.S. and Chitra, L., 2022, April, ‘Bidirectional SEPIC-ZETA converter for battery based grid-tied PV system’, In AIP Conference Proceedings (Vol. 2405, No. 1, p. 040006). AIP Publishing LLC.

 https://doi.org/10.37896/pd91.4/91489

8. Li, C., Zhang, L., Ou, Z., Wang, Q., Zhou, D. and Ma, J., 2022, ‘Robust model of electric vehicle charging station location considering renewable energy and storage equipment’, Energy, vol.238, p.121713.
9. Lin, X., Li, K. and Wang, L., 2022, ‘A driving-style-oriented adaptive control strategy based PSO-fuzzy expert algorithm for a plug-in hybrid electric vehicle’, Expert Systems with Applications, vol.201, p.117236.
10. Majji, R.K., Prakash Mishra, J. and Dongre, A.A., 2022, ‘Model predictive control of solar photovoltaic based microgrid with composite energy storage’, International Journal of Circuit Theory and Applications.
11. Ni, J., Hu, J. and Xiang, C., 2018, ‘Control-configured-vehicle design and implementation on an X-by-wire electric vehicle’ IEEE Transactions on Vehicular Technology, vol.67, no.5, pp.3755-3766.
12. Priyadarshi, N., Bhaskar, M.S., Sanjeevikumar, P., Azam, F. and Khan, B., 2022, High-power DC-DC converter with proposed HSFNA MPPT for photovoltaic based ultra-fast charging system of electric vehicles’, IET Renewable Power Generation.
13. Rezaei, A., Burl, J.B., Rezaei, M. and Zhou, B., 2018, ‘Catch energy saving opportunity in charge-depletion mode, a real-time controller for plug-in hybrid electric vehicles’, IEEE Transactions on Vehicular Technology, vol.67, no.11, pp.11234-11237.
14. Saravanan, S., Pandiyan, P., Chinnadurai, T., Tiwari, R. and Prabaharan, N., 2022, ‘Overview of Bidirectional DC–DC Converters Topologies for Electric Vehicle and Renewable Energy System’, In DC—DCConverters for Future Renewable Energy Systems (pp. 433-458), Springer, Singapore.
15. Shetty, D., Rao, S. and Rohan, K.U., 2022, ‘Performance Enhancement of PV Systems Using Adaptive Reference PI Controller’, International Journal of Research in Engineering, Science and Management, vol.5, no. 5, pp.212-215.
16. Shilaja, C., Kiran, S.R., Murali, M., Moinuddin, S.K., Navani, K., Yousuf, S. and Harshith, M., 2022, ‘Design and analysis of global optimization methods for proton exchange membrane fuel cell powered electric vehicle system with single switch DC-DC converter’, Materials Today: Proceedings, vol.52, pp.2057-2064.
17. Shoeibi, S., Kargarsharifabad, H., Mirjalily, S.A.A., Sadi, M. and Arabkoohsar, A., 2022, ‘A comprehensive review of nano-enhanced phase change materials on solar energy applications’, Journal of Energy Storage, vol.50, p.104262.
18. Thota, P., Bhimavarapu, A.R. and Chintapalli, V.B.R., 2022, ‘Participation Factor based analysis of PVSC type Multi-Input Zeta-SEPIC dc-dc converter’, COMPEL-Theinternational journal for computation and mathematics in electrical and electronic engineering.
19. Titus, F., Thanikanti, S.B., Deb, S. and Kumar, N.M., 2022, ‘Charge Scheduling Optimization of Plug-In Electric Vehicle in a PV Powered Grid-Connected Charging Station Based on Day-Ahead Solar Energy Forecasting in Australia’, Sustainability, vol.14, no.6, p.3498.

20. Trinh, H.A., Truong, H.V.A. and Ahn, K.K., 2022, 'Development of Fuzzy-Adaptive Control Based Energy Management Strategy for PEM Fuel Cell Hybrid Tramway System', Applied Sciences, vol.12, no.8, p.3880.
21. Wang, B., Dehghanian, P., Wang, S. and Mitolo, M., 2019, 'Electrical safety considerations in large-scale electric vehicle charging stations', IEEE Transactions on Industry Applications, vol. 55, no.6, pp.6603-6612.
22. Xiaoluan, Z., Farajian, H., Xifeng, W. and Ohshima, K., 2022, 'Scheduling of renewable energy and plug-in hybrid electric vehicles based microgrid using hybrid crow—Pattern search method', Journal of Energy Storage, vol. 47, p.103605.
23. Xu, B., Yan, Z., Zhou, W., Zhang, L., Yang, H., Liu, Y. and Liu, L., 2022, 'A Bi-directional Integrated Equalizer Based on the Sepic-Zeta Converter for Hybrid Energy Storage System', IEEE Transactions on PowerElectronics.
24. Zhang, D., Liu, G., Zhou, H. and Zhao, W., 2018, 'Adaptive sliding mode fault-tolerant coordination control for four-wheel independently driven electric vehicles' IEEE Transactions on Industrial Electronics, vol. 65, no.11, pp.9090-9100.